AACVD synthesis of catalytic gold nanoparticle-modified cerium(IV) oxide thin films

Meghan Evans[1], Francesco Di Maggio[1], Chris Blackman[*,1], Gopinathan Sankar[1]

[1] Department of Chemistry, University College London, 20 Gordon Street, London, WC1H 0AJ, UK

Received ZZZ, revised ZZZ, accepted ZZZ
Published online ZZZ (Dates will be provided by the publisher.)

Keywords Please provide about four verbal keywords for your manuscript.

* Corresponding author: e-mail c.blackman@ucl.ac.uk, Phone: +44 207 679 4703, Fax: +44 207 679 7463

Co-deposition of $Ce(dbm)_4$ and NH_4AuCl_4 precursors in acetone at 500°C *via* AACVD results in deposition of crystalline CeO_2 thin films containing/decorated with metallic gold. These particles are estimated to be ~ 70 nm in size via optical methods. Preliminary testing of catalytic activity showed the materials were surprisingly catalytically active given the very small amounts of gold present and the large estimated particle size, although the presence of smaller catalytically active particles could not be discounted.

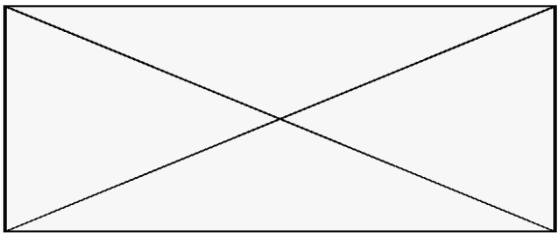

This is the caption of the **optional** abstract figure. If there is no figure here, the abstract text should be divided into both columns.

1 Introduction The catalytic activity of gold nanoparticles (NP) increases when supported on oxide thin films, for example TiO_2 and Al_2O_3,[1] with the support playing a critical part in the activity.[2] Cerium oxide (CeO_2) has been found to increase the catalytic activity of supported gold NP in CO oxidation by two orders of magnitude in comparison to TiO_2 or Fe_2O_3 supports due to improved dispersion of gold, and the use of an Au/CeO_2 catalyst in the water-gas shift reaction has been shown to be more active than the current commercial catalysts.[3]

Vapour synthesis of gold nanoparticles (NP), e.g. via chemical vapour deposition (CVD), offers advantages over wet-chemical techniques; it circumvents several steps associated with solution methods such as washing, drying, calcination and reduction, and can avoid changes in metal dispersion that can occur during high temperature calcination or reduction steps.[4]

For deposition of CeO_2 the typically low volatility of cerium CVD precursors has led to investigation of a wide-range of fluorinated β-diketonates in MOCVD,[5-9] although these tend to lead to fluorine incorporation.[10] An alternative strategy for overcoming low volatility is to introduce the precursor as a solution droplet, and this has been utilized for use of cerium nitrate in electrospray CVD,[11] and for use of $Ce(thd)_4$ (thd = 2,2,6,6-tetramethyl-3,5-heptanedionato) in aerosol-assisted CVD.[12-14]

Through extensive experience in the use of AACVD for co-depositing metal NP supported on metal oxides,[15,16] we have previously observed that use of $HAuCl_4$ or H_2PtCl_6 as metal precursors, which in terms of decomposition characteristics are excellent, can be incompatible in solution with metal alkoxide and β-diketonates when used in a convenient one-pot system containing both precursors. Strategies to alleviate this involve use of more robust metal oxide precursors, for instance the use of $Bi(dbm)_3$ (dbm = dibenzylmethanato) instead of $Bi(thd)_3$,[17] or less acidic metal precursors such as metal phosphine cluster complexes[18] or NH_4AuCl_4.[19] In this paper we describe the use of $Ce(dbm)_4$ and NH_4AuCl_4 precursors in a one-pot AACVD strategy for co-deposition of gold NP-modified CeO_2, and report on its catalytic activity for a test oxidation reaction of benzyl alcohol to benzaldehyde.

2 Results and Discussion

2.1 Experimental $Ce(dbm)_4$ was synthesised by adaption of the method for synthesis of $Ce(thd)_4$,[5] ^{1}H NMR δ/ppm ($CDCl_3$, 300 MHz): 6.70 (s, 1H, (C*H*)), 7.4 (m, 9H, C_6H_5– plus $CDCL_3$ peak), 8.0 (d, 4H C_6H_5-) (^{1}H NMR dibenzoylmethane δ/ppm ($CDCl_3$, 300 MHz): 6.9 (s, 1H), 7.5 (m, 6H), 8.0 (m, 4H), 16.9 (s, 1H), indicating the loss of the H from the alcohol group after coordination). FT-IR cm^{-1}: 1588, 1512, 1473, 1374, 1285, 1221, 1063, 1022, 938, 784, 747, 712, 682, 603, 509, 429 (FT-IR cm^{-1} dibenzoylmethane: 11462, 1308, 1227, 998, 752, 704, 678, 607, 493).

The general AACVD method was as follows: 50 mg $Ce(dbm)_4$ was dissolved in 20 cm^3 acetone (and 1 mg NH_4AuCl_4 added for gold modified samples), a piezoelectric ultrasonic atomizer (Johnson Mathey Liquifog, 1.6 MHz) was used to generate an aerosol from the precursor mixture, which was then carried to the heated substrate (500°C) by an N_2 gas flow (200 cm^3/min). The substrates used were plain glass microscope slides.

Thermal Gravimetric analysis (TGA) was carried out using a NETZSCH STA–449C Jupiter balance under helium flow. X-ray diffraction measurements were completed using a Bruker D8 X-ray diffractometer with $CuK_\alpha1$ and $CuK_\alpha2$ radiation of wavelengths 0.154056 nm and 0.154439 nm respectively, emitted with an intensity ratio of 2:1. A voltage of 40 kV and current of 40 mA were used. The diffraction pattern was recorded over the range 2θ = 10-60°. Scanning Electron Microscopy (SEM) was performed using a JEOL JSM-6301F Field Emission Scanning Electron Microscope at an accelerating voltage of 5 keV and Energy Dispersive Analysis by X-Rays (EDAX) was performed using an attached Oxford Instruments INCA Energy EDAX system. X-ray photoelectron spectroscopy (XPS) was carried out using a Thermo K-Alpha spectrometer in constant analyser energy mode and monochromated Al Kα radiation. Survey scans were collected over the 0 – 1400 eV binding energy range with 1 eV resolution and a pass energy of 200eV. Higher resolution scans (0.1 eV) were also collected at a pass energy of 50 eV. Data was processed using CasaXPS. Raman spectra were collected using a Renishaw ramascope and UV/Visible/Near IR spectra were taken using a Perkin Elmer Fourier transform Lambda 950 UV/Vis spectrometer over a wavelength range of 300 nm to 2500 nm in the transmission mode.

Catalytic testing was carried out using a Multimax Multiple Automatic Lab described previously,[20] by immersing films in a solution of 4.5 cm^3 benzyl alcohol, 11.4 cm^3 tetra-butyl hydrogen peroxide (TBHP) and 10 cm^3 decane, and stirred at 94ºC for 4 hours. Samples were collected for analysis at 0, 15, 30, 45, 60, 120, 180 and 240 minutes. The samples were analysed using a PerkinElmer Clarus 500 Gas Chromatograph with a flame ionization detector to investigate the conversion of benzyl alcohol and the selectivity to the desired product, benzaldehyde.

2.2 Results and Discussion TGA data for $Ce(dbm)_4$ (Figure 1) showed the onset of first mass loss at ~ 200°C, coincident with an endotherm in the DSC. This weight loss is attributed to volatilization of the precursor slightly lower than the value found previously for $Ce(thd)_4$ of 250°C.[21] Accelerated weight loss is observed at ~ 400°C, coinciding with an exotherm in the DSC and this is attributed to initial decomposition of the precursor, which continues across three distinct steps until 550°C. Assuming no decomposition prior to 400°C, the total % weight loss during decomposition is therefore approximately 50% whereas the mass loss required for complete conversion of $Ce(dbm)_4$ to CeO_2 is 83%, indicating incomplete decomposition (carbon contamination) may be expected during CVD. NH_4AuCl_4 decomposes in a single principle step (Figure 1) losing 43% of its mass by 300°C, although an initial loss of mass is observed from 50°C attributed to loss of water of crystallisation. The mass loss required for complete conversion to pure gold is 55%, indicating residual chloride contamination is possible. In contrast $HAuCl_4$ exhibits two main stages of weight loss after loss of water of crystallization up to 135°C, with the first step up to 220°C corresponding to the loss of HCl and Cl_2 and the second step up to 294°C attributed to the disproportionation of AuCl producing Au and Cl_2.

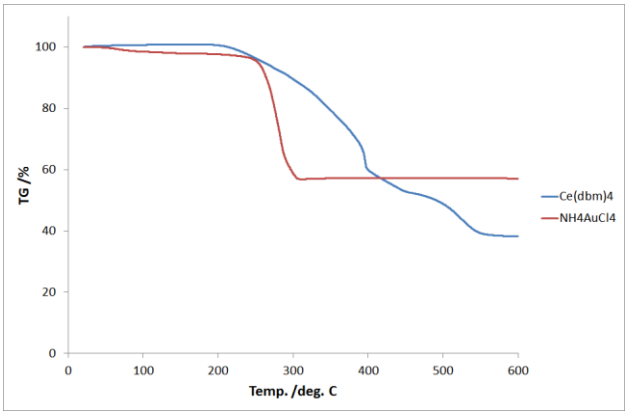

Figure 1 TGA data for $Ce(dbm)_4$ (blue line) and NH_4AuCl_4 (red line).

Deposition using $Ce(dbm)_4$ alone produced pale cream opaque films. XRD analysis showed good agreement for cerium oxide (Fm-3m space group , a = b = c = 5.507(3) Å; ICDD card no. 01-081-0792 a = b = c = 5.4124 Å) (Figure 2).[22]

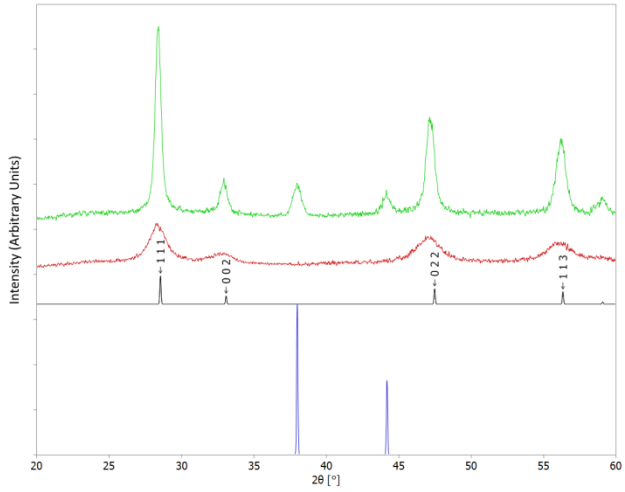

Figure 2 XRD patterns of films deposited at 500°C from $Ce(dbm)_4$ only (red line) or $Ce(dbm)_4/NH_4AuCl_4$ (green line). Literature patterns for CeO_2 (black) and Au (blue) are also shown.

Raman spectroscopy shows a peak centred at 456 cm^{-1} (Figure 3), in accordance with the literature value for CeO_2 (465 cm^{-1}). [23]

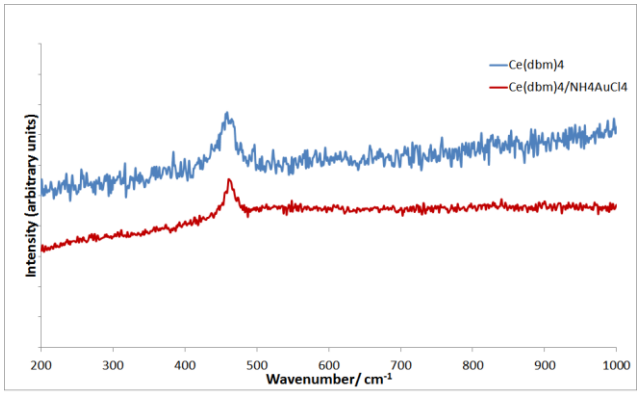

Figure 3 Raman spectra of films deposited at 500°C from $Ce(dbm)_4$ only (blue line) or $Ce(dbm)_4/NH_4AuCl_4$ (red line)

UV-vis spectra of a film deposited at 500°C is shown in Figure 4a, compared to a blank glass substrate (Figure 4c; peaks at ~ 850 nm are due to a detector change on the instrument). The band-gap (Eg) of a semiconductor can be inferred from its UV-Vis spectra using the following equation:

$$(\alpha h\nu)n = A(h\nu - Eg)$$

Where α corresponds to the absorption coefficient, hυ is the photon energy, and n represents the index which depends on the electronic transition of the semiconductor.[24] Estimation of the bandgap from the band edge for the CeO_2 film indicates a value of ~ 3.1 eV, in good agreement with the literature value of 3.15 eV.[25]

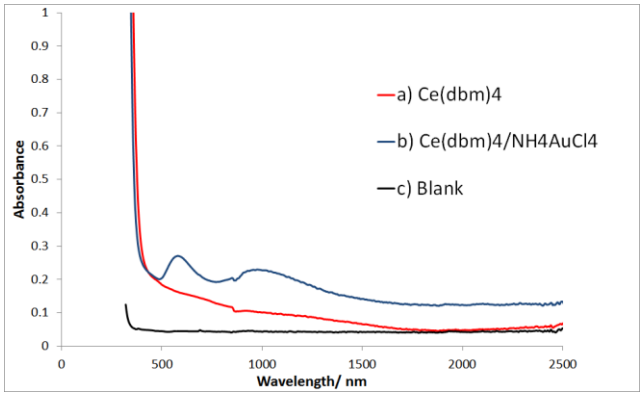

Figure 4 UV-vis spectra of films deposited at 500°C from a) $Ce(dbm)_4$ only (red line), b) $Ce(dbm)_4/NH_4AuCl_4$ (blue line) compared to, c) blank glass substrate (black line)

Bêche et al.[26] carried out an XPS study of cerium oxide and mixed cerium oxides assigning six peaks, corresponding to pairs of spin-orbit doublets (labelled v and u), in the Ce $3d_{3/2,5/2}$ spectrum. Analysis of a film deposited at 500°C (Figure 5) found peaks at 916.8 (u'''), 898.1 (v'''), 906.4 (u''), 887.8 (v''), 901.2 (u) and 882.6 (v). The u''' (916.9), v''' (898.3) and the u (901.3), v (882.7) peaks are in very good agreement with the literature values (shown in brackets) although the u'' (907.3), v'' (888.5) peaks are noticeably different. The satellite u''' peak is indicative of the presence of Ce(IV).

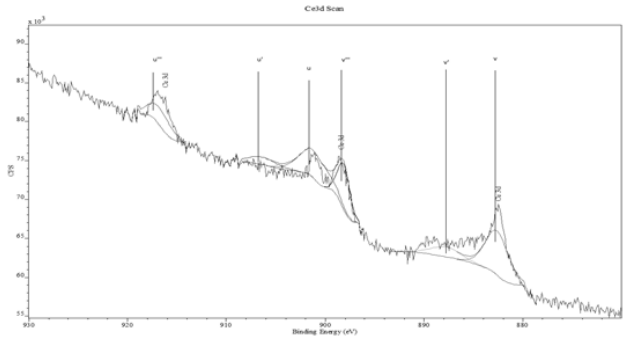

Figure 5 XPS spectrum of film deposited at 500°C from $Ce(dbm)_4$ only

SEM analysis showed the films were comprised of separated grains comprised of agglomerates of smaller crystallites (Figure 6A)

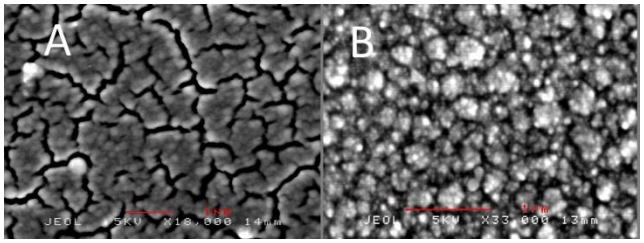

Figure 6 SEM image of film deposited at 500°C from $Ce(dbm)_4$ only (A) or $Ce(dbm)_4/NH_4AuCl_4$ (B) (in both images scale bar in red depicts 1 μm)

Addition of NH_4AuCl_4 into the reaction mixture caused deposition of blue/black coloured films. Annealing in air at 500°C resulted in films with a deep blue colouration. XRD analysis showed evidence of crystalline CeO_2 (Fm-3m space group , a = b = c = 5.492(2) Å) as previously and also the presence of metallic gold (Fm-3m space group, a = b = c = 4.070(1) Å; ICDD card no. 00-04-0784 a = b = c = 4.0786 Å) (Figure 2). Raman spectroscopy was indicative of the presence of CeO_2 (Figure 3). EDX gave a Ce/Au weight % ratio of 10:1, very close to the weight ratio of the metals in the precursor solution. SEM (Figure 6B) showed a change in morphology compared to films deposited in the absence of NH_4AuCl_4, appearing rougher with more defined island-morphology. XPS analysis agreed closely with literature values for CeO_2 with peaks at 917.0 (u'''), 898.4 (v'''), 907.0 (u''), 888.4 (v''), 901.3 (u) and 882.7 (v) eV. Peaks were also observed in the Au 4f region with binding energies 83.7 and 87.4 eV, in good agreement with the literature values of 84.0, 87.9 eV for metallic gold,[27] demonstrating the presence of gold at the surface of the co-deposited films. Comparison with EDX data showed no evidence for surface segregation of Au with almost identical Ce/Au ratios found via both techniques.

UV-vis spectra (Figure 4) displayed a broad absorbance between 500 and 650 nm, attributed to the surface plasmon resonance of the gold particles, with the peak centre at ~ 580 nm. Estimation of gold particle size from the peak absorbance of the plasmon observed using UV-vis spectroscopy (Figure 4), using multipole scattering theory as described by Haiss *et al*[28] and assuming the gold particles were spherical and uncoated and the refractive index of the medium in contact with the particles was dominated by CeO_2 (~2.2 at 550 nm)[29], gave a value of 70 nm. This is far in excess of the desired size for catalytic gold nanoparticles, for instance Haider et al[30] investigated the effect gold nanoparticle size had on the catalytic activity of Au/TiO_2 and Au/CeO_2 where the gold particles ranged in size from 1.3-11.3 nm and it was found that the highest catalytic activity emerged for an average particle size of 6.9 nm. However the gold loading in these experiments was high (10 wt.% Au compared to Ce in precursors) due to practical limitations in preparing solutions at lower concentrations and this is the likely cause of the large particle size since we have previously observed much smaller particles when using $HAuCl_4$ or H_2PtCl_6.[31] We also note that our analysis does not preclude the presence of undetectable gold particles within the catalytically active range identified by Haider, but difficulty with sample preparation precluded identifying these using electron microscopy.

Films deposited from $Ce(dbm)_4$ (CeO_2) and $Ce(dbm)_4/NH_4AuCl_4$ (Au/CeO_2) were tested for catalytic activity during oxidation of benzyl alcohol (Table 1). The selective catalytic oxidation of hydrocarbons to their respective aldehydes is a major challenge for industry and reactions are frequently performed at very low conversion rates in order to avoid the formation of carboxylic acids.[32] Oxidation of benzyl alcohol to benzaldehyde is a useful test reaction as it is easily over-oxidised to benzoic acid and therefore provides a direct measure of the selectivity of the catalyst. It is clear that both the plain glass substrate and CeO_2 thin film had no measurable activity during the period of test. The Au/CeO_2 film tested showed measurable conversion and turnover number (TON), with very good selectivity towards benzaldehyde. However it should be noted that the amount of reagents used in this reaction were designed to be used with 200-250 mg gold as catalyst but the amount of active catalyst present in our films being significantly lower than this hence the low total conversion (average amount of material in 2 cm^2 thin film, the maximum size that could fit in reactor, is 2 mg and then by using EDX the amount of gold in the sample can be estimated). The TON value is greater than a sample of gold nanoparticles supported on SiO_2 prepared *via* solution-phase impregnation/calcination (TON 580), although lower than gold nanoparticles supported on nanostructured tungsten oxide (~20000, although the surface area here is expected to be considerably lower).[18]

Table 1. Catalytic performance of film deposited from $Ce(dbm)_4$ and NH_4AuCl_4 at 500°C.

Sample	Conversion to oxidized products %	TON (gold only)	Selectivity to benzaldehyde %	Estimated Mass Gold from EDX /mg
Plain Glass	0.0	-	0.0	0.0
CeO_2	0.0	-	0.0	0.0
Au/CeO_2	8.2	3600	91.1	0.2

3 Conclusions Co-deposition of $Ce(dbm)_4$ and NH_4AuCl_4 precursors in acetone at 500°C *via* AACVD results in deposition of crystalline CeO_2 thin films containing/decorated with metallic gold. These particles are estimated to be ~ 70 nm in size via optical methods. Prelimi-

nary testing of catalytic activity showed the materials were surprisingly catalytically active given the very small amounts of gold present and the large estimated particle size (although the presence of smaller particles cannot be discounted). It has been found previously that higher catalytic performance is observed in CVD deposited materials than those produced using solution-phase methods and these results may reflect this.[33] Future work is aimed at reducing the gold loading, and in particular reducing the gold particle size, and observing the effect on the catalytic activity.

Acknowledgements An acknowledgement may be placed at the end of the article.

References

[1] M. Comotti, W. Li, B. Spliethoff, F. Schüth, J. Am. Chem. Soc., **128**, 917 (2006).
[2] A. Kozlov, A. Kozlova, H. Liu, Y. Iwasawa, Appl Catal. A General, 182, 93 (1999).
[3] S. Senanayake, D. Stacchiola, J. Evans, M. Estrella, L. Barrio, M. Pérez, J. Hrbek, J. Rodriguez, J. Catal., **271**, 392 (2010).
[4] A. E. Aksoylu, J. L. Faria, M. F. R. Pereira, J. L. Figuieredo, P. Serp, J. -C. Hierso, R. Feurer, Y. Kihn, P. Kalck, Appl. Catal A: General, **243**, 357 (2003).
[5] M. Becht, T. Gerfin, K-H. Dahmen, Chem. Mater., **5**, 137 (1993).
[6] I. Baxter, J. Darr, M. Hursthouse, K. Abdul Malik, J. McAleese, D. Michael, P. Mingos, Polyhedron, **17**, 1239 (1998).
[7[K. Pollard, H. Jenkins, R. Puddephatt, Chem. Mater., **12**, 701 (2000).
[8] G. Malandrino, R. Lo Nigro, C. Benelli, F. Castelli, I. Fragalà, Chem. Vap. Deposition, **6**, 233 (2000).
[9] R. Lo Nigro, G. Malandrino, I. Fragalà, Chem. Mater., **13**, 4402 (2001).
[10] J. McAleese, J. Plakatauros, B. Steele, Thin Solid Films, **280**, 152 (1996).
[11] M. Wei, K. Choy, J. Crystal Growth, **284**, 464 (2005).
[12] K. Frölich, J. Šouc, D. Machajdĩk, A. Kobzev, F. Weiss, J. Senateur, K. Dahmen, J. Physique IV, **5**, 533 (1995).
[13] C. Xia, T. Ward, R. Schwartz, Chem. Vap. Deposition, **2**, 48 (1996).
[14] M. Siadati, T. Ward, J. Martus, P. Atanasova, C. Xia, R. Schwartz, Chem. Vap. Deposition, **3**, 311 (1997).
[15] C. Navío, S. Vallejos, T. Stoycheva, E. Llobet, X. Correig, R. Snyders, C. Blackman, P. Umek, X. Ke, G. Van Tendeloo, C. Bittencourt, Mat. Chem. Phys., **134**, 809 (2012).
[16] T. Stoycheva, S. Vallejos, J. Calderer, I. Parkin, C. Blackman, X. Correig, Procedia Engineering, **5**, 131 (2010).
[17] S. J. A. Moniz, D. Bhachu, C. S. Blackman, A. J. Cross, S. Elouali, D. Pugh, R. Quesada Cabrera, S. Vallejos, Inorganica Chimica Acta, **380**, 328 (2012).
[18] A. Molkenova, R. Sarip, S. Sathasivam, P. Umek, S. Vallejos, C. Blackman, G. Hogarth, G. Sankar, Sci. Technol. Adv. Mater., **15**, 065004 (2014).
[19] F. Di Maggio, M. Ling, A. Tsang, J. Covington, J. Saffell, C. Blackman, J. Sens. Sens. Syst., **3**, 325 (2014).
[20] A. Welch, N. Shiju, I. Watts, G. Sankar, S. Nikitenko, W. Bras, Catal. Lett., **105,** 179 (2005).
[21] M. Leskela, R. Sillanpaa, L. Niinisto, M. Tiitta, Acta Chem. Scand., **45**, 1006 (1991).
[22] M. Wolcyrz, L. Kepinski, J. Sol. State Chem., **99**, 409 (1992).
[23] J. Twu, C. Chuang, K. Chang, C. Yang, K. Chen, Applied Catalysis B: Envir., **12**, 309 (1997).
[24] J. Tauc, R. Grigorovici, A. Vancu, physica status solidi (b), **15**, 627 (1966).
[25] F. Zhang, Q. Jin, S. Chan, J. Appl. Phys., **95**, 4319 (2004).
[26] E. Bêche, P. Charvin, D. Perarnau, S. Abanandes, G. Flamant, Sur. Inter. Anal., **40**, 264 (2008).
[27] P. Bera, M. Hedge, Catal. Lett., **79**, 75 (2002).
[28] W. Haiss, N. T. K. Thanh, J. Aveyard, D. G. Fernig, Anal. Chem., **79**, 4215 (2007).
[29] G. Hass, J. B. Ramsey, R. Thun, J. Optical Soc. Am., **48**, 324 (1958).
[30] P. Haider, B. Kimmerle, F. Krumeich, W. Kleist, J. Grunwaldt, A. Baiker, Catal. Lett., **125**, 169 (2008).
[31] S. Vallejos, P. Umek, T. Stoycheva, F. Annanouch, E. Llobet, X. Correig, P. De Marco, C. Bittencourt, C. Blackman, Adv. Funct. Mater., **23**, 1313 (2013).
[32] K. R. Seddon, A. Stark, Green Chem., **4**, 119 (2002).
[33] V. Garcia, Mater. Sci. Eng., **20**, 012001 (2011).